Werk

Jahr: 1975
Kollektion: fid.geo
Signatur: 8 Z NAT 2148:41
Digitalisiert: Niedersächsische Staats- und Universitätsbibliothek Göttingen
Werk Id: PPN1015067948_0041
PURL: http://resolver.sub.uni-goettingen.de/purl?PPN1015067948_0041

LOG Id: LOG_0046
LOG Titel: Noise variance fluctuations and earthquake detectability
LOG Typ: article

Übergeordnetes Werk

Werk Id: PPN1015067948
PURL: http://resolver.sub.uni-goettingen.de/purl?PPN1015067948
OPAC: http://opac.sub.uni-goettingen.de/DB=1/PPN?PPN=1015067948

Contact

Niedersächsische Staats- und Universitätsbibliothek Göttingen
Georg-August-Universität Göttingen
Platz der Göttinger Sieben 1
37073 Göttingen
Germany
Email: gdz@sub.uni-goettingen.de

J. Geophys. 41, 289–302, 1975

Noise Variance Fluctuations and Earthquake Detectability

O. Steinert, S. Husebye, H. Gjøystdal

NORSAR, Kjeller

Received October 14, 1974; Revised Version February 3, 1975

Abstract. Shimshoni (1972) observed diurnal variations in earthquake occurrence as reported by NOAA. This effect, which is generally explained in terms of noise level fluctuations, manifests itself at the NORSAR array in Norway. However, large diurnal variations are also observed in the number of pure noise detections (false alarms) reported by the NORSAR on-line detector. This has to be attributed to changes in the statistical properties of the noise, as the detector, having a fixed detection threshold, is insensitive to fluctuations in the noise level. Such changes are not likely to be reflected accurately in the inherently subjective detectability based on visual inspection of seismograms.

Two indicators for estimating the false alarm rate have been considered; the most successful, called the noise stability, is defined as the ratio between squared noise average and noise variance. A relation between detection threshold, stability and false alarm rate has been established which makes it possible to fix the false alarm rate and let the threshold 'float', i.e., vary as function of the noise stability. It is shown that implementation of a floating detection threshold will generally improve signal detectability by about 4% relative to a fixed threshold operation. Other advantages are avoidance of system saturation during extremely noisy time intervals and a more economical use of the computer capacity with respect to load caused by diurnal false alarm rate. The treatment presented is applicable to other types of on-line signal detection problems.

Key words: Noise Variance Fluctuations – Earthquake Detection – NORSAR Array – Fixed and Floating Event Detector Threshold.

Introduction

Earthquake occurrence has been thought to be a response of the earth to periodic stresses connected with orbital frequencies of the sun-earth-moon system. Recently, in a statistical analysis of three years of NOAA (U.S. National Oceanic and Atmospheric Administration) earthquake data, Shimshoni (1971) found that the earthquake activity was highest during local night time, and in consequence postulated that the sun has an effect on seismicity. However, according to Davis (1972), Flinn *et al.* (1972) and Knopoff and Garder (1972) this conjecture is based on an incorrect interpretation of the raw NOAA data, as the effect on diurnal noise level fluctuations on the global network seismic event detection capability is not taken into account. It is well-established that short period seismic noise is significantly greater during day than night, the effect being more pronounced where cultural sources contribute significantly to the noise background. In a reply to the critical analyses, Shimshoni (1972) concedes that the diurnal noise fluctuations are very important for the interpretation of his original results, but he expresses doubt as to whether this effect could explain all the observed diurnal variation in earthquake occurrence. Not unexpectedly, Bungum and Ringdal (1973) found that the seismicity as observed by

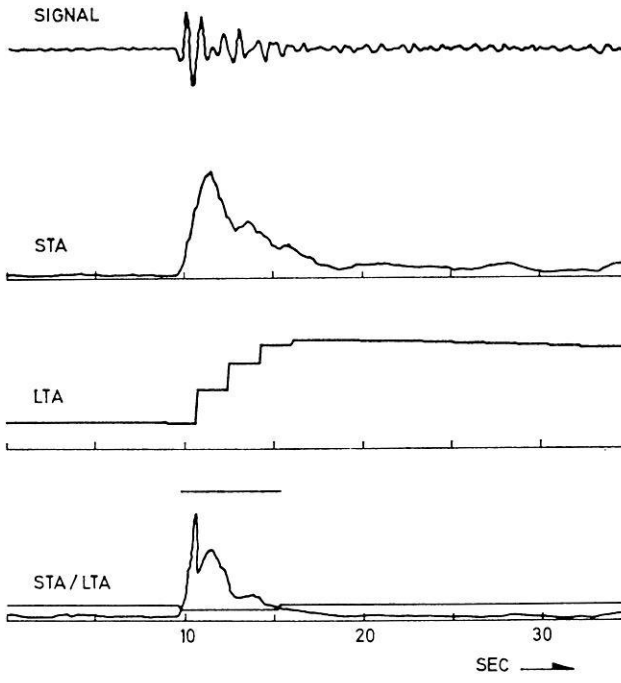

Fig. 1. Beam, STA, LTA and STA/LTA for earthquake from Tsinghai, China; arrival time Jan 27 1970, 10.59.40.1 filtered 1.0–3.0 Hz. STA integration time is 1.8 s, and LTA computation rate is 5/9 Hz. The short line above the STA/LTA curve indicates detection state, and the line crossing the curve is the threshold

the NORSAR array exhibits a clear diurnal variation. However, they also found that the number of times the array's automatic event detector was triggered was much larger during local night time than day time (see Fig. 1). The latter result indicates that not only the noise level but also the noise variance or noise field variations must be considered when discussing the detectability of small earthquakes.

The aim of this study is to investigate the effect of noise field variations on the earthquake-reporting performance of the NORSAR array. Also, ways to improve its event detectability will be considered. The reasons for using the NORSAR installation are numerical convenience and, more importantly, to avoid the subjectivity involved in visual seismogram readings. We remark, however, that the problems and principles involved are of a general type, and are relevant in a variety of on-line signal detectors.

Seismic Array Detector Design and Noise Characteristics

The large arrays LASA and NORSAR represent in general the most efficient tool available for detecting small seismic events. The basic operational principle of the array is beamforming; the array is regularly steered towards a large number of predetermined points distributed throughout the active seismic regions. Due to the large amount of data generated by NORSAR's 132 short period seismometers,

an on-line detector is required for the surveillance task of the array. The most commonly used detector is based on a continuous comparison between a certain parameter η and a present detection threshold, η being the ratio between the linear array beam power measured in a short (STA) and a long (LTA) time window. (The NORSAR array and its operational procedures are described by Bungum *et al.* (1971) and Bungum and Husebye (1974).

The problem of declaring a signal detection represents a hypothesis test based on the test statistic η: declare a detection whenever η is equal to or exceeds a present detection threshold (TH), i.e., choose hypothesis H_1. Otherwise, decide that H_1 is false, i.e., hypothesis H_0 is chosen. Symbolically,

$$\eta \underset{H_0}{\overset{H_1}{\gtrless}} \mathrm{TH} \tag{1}$$

This binary decision model has two error conditions; the false alarm (FA) or choosing H_1 when H_0 is true, and the missed detection (MD) or choosing H_0 when H_1 is true. The test statistic itself is given in Eq. (1), while the definitions of the STA and LTA parameters are

$$\mathrm{STA}(t) = \sum_{i=t}^{t+L-1} |a(i)| \tag{2}$$

$$\mathrm{LTA}(t') = (1-2^{-5}) \cdot \mathrm{LTA}(t'-\mathrm{L}) + \mathrm{STA}(t'-\mathrm{L})/2 \tag{3}$$

Here t and t' are STA and LTA sampling times, $a(i)$ is array beam amplitude, and L is STA integration window length, typically 1.5 sec. The η and STA sampling rate is 2 Hz while the much more slowly varying parameter LTA has a 2/3 Hz sampling rate. A schematic representation of the array detector is shown in Fig. 1. The STA operation is equivalent to time domain filtering of the rectified beam, and its frequency response is shown in Fig. 2. Additional noise suppression beside that of beamforming is obtained by prefiltering with a 3rd order Butterworth bandpass filter. The possibility of seismic signal recording is tested around $50 \cdot 10^6$ times every day, although only one third of these tests can be considered independent due to time and/or spatial overlaps of the STA parameter. It is important to note that the detector is working on the very tail of the η or STA distribution function, as the TH-value is roughly the mean value plus 6—8 times the standard deviation of the STA samples.

The design of the NORSAR detector is not derived from any optimum criteria (Helstrøm, 1968) because the noise amplitude probability function is not exactly known and the noise exhibits both diurnal and seasonal fluctuations. This means that the test statistic η is unstable, which implies a variable false alarm probability for a given threshold. An example of the non-stationarity of the noise field is given in Fig. 3. During local night time the noise decreases, thus explaining why the number of events reported increases. Flinn *et al.* (1972) have obtained similar results for the

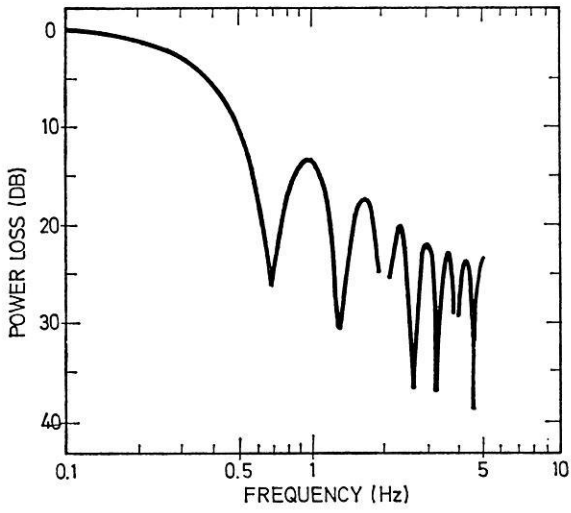

Fig. 2. Response curve for the STA-operator. Filter length is 1.5 sec

LASA array. However, during night the number of false alarms also increases (see Fig. 4), and this phenomenon must be attributed to changes in the noise character. The reason is that the false alarm rate is independent of the noise level or the STA-value itself, but does depend on its variance. In terms of the binary decision model incorporated in the array's detector, this means also that the probability of a missed detection is larger during day time. The above phenomenon is fairly easy to explain in terms of noise spectra fluctuations. During night time the relatively low frequency microseismic noise dominates, while high frequency cultural noise is added during day time (see Fig. 3). From the theoretical studies of Rice (1944) and Cartwright and Longuet-Higgins (1956) the probability density distribution of noise maxima is expected to vary accordingly, i.e., between Rayleigh and Gaussian distributions. Also during heavy microseismic storms the noise spectra change. A theoretical explanation of the corresponding variations in the false alarm rate has been given. by Lacoss (1972).

Data Analysis and Results

In the previous sections it was demonstrated that an array's event detectability, i.e., its ability to report 'true' seismic signals, does depend both on the noise level and the noise character or, in other words, the unstable noise probability function. Moreover, when a fixed detection threshold is used, the probability of a missed detection is higher during day time than night time. One possible way to improve the event detectability is to exercise a better control with the false alarm rate, i.e., to use a floating threshold value in the automatic signal detector. This point will be discussed in detail in a later section.

Two different false alarm indicators have been analyzed. The first, here denoted ε, was suggested by Cartwright and Longuet-Higgins (1956) in their study of distribution functions of ocean wave maxima. In general, ε is a measure of the RMS

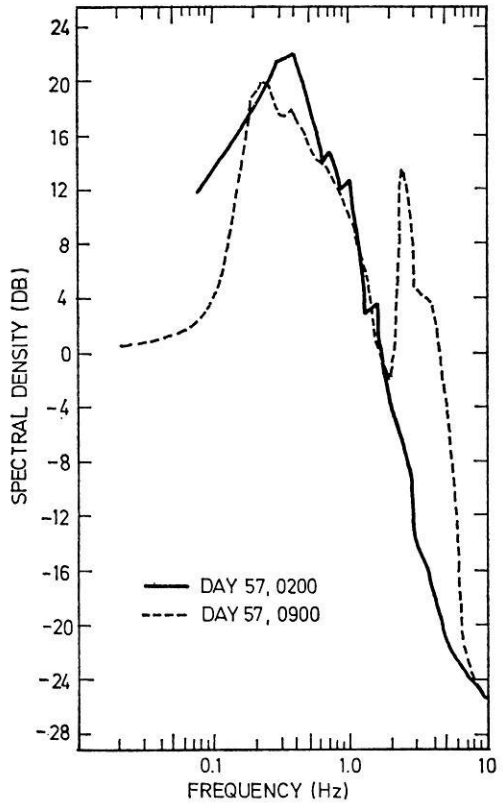

Fig. 3. Power spectral densities for two single sensor noise samples showing the difference between typical night- and daytime situations in 1973

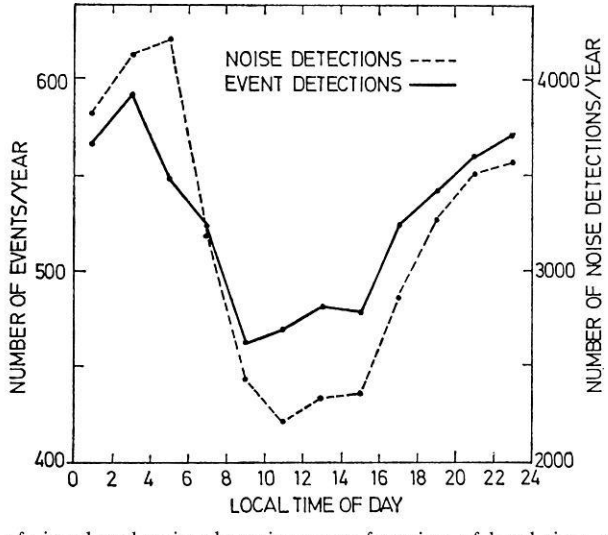

Fig. 4. Number of signal and noise detections as a function of local time of day, obtained by Bungum and Ringdal, 1974

width of the energy spectrum, and was found to vary between zero and one as the probability density function of the waveform maxima changed from Rayleigh to Gaussian. ε is defined as

$$\varepsilon^2 = \frac{m_0 m_4 - m_2^2}{m_0 m_4} \tag{4}$$

or

$$\varepsilon^2 = 1 - \frac{N_0^{+2}}{N_1} \tag{5}$$

where m_i is the spectral moment of i-th order, N_0^+ is the density of zero line upcrossings, and N_1 the density of maxima in a certain time window. Due to its computational simplicity, Eq. (5) was used in the analysis.

The other false alarm indicator considered, in the following called the noise stability, is defined as:

$$S = \frac{\eta^2}{\sigma^2(\eta)} \approx \frac{\overline{STA}^2}{\sigma^2(\overline{STA})} \tag{6}$$

where $\eta = STA/LTA$ and the bar indicates averaging. The S-term approximation used above will not introduce significant errors as the LTA-term varies very slowly. The stability S is a generalized measure of the spread in the η observations and is likely to be a sensitive indicator for phenomena of the type investigated here (Lacoss, 1972).

The signal detector at NORSAR comprises 318 array beams, of which a subset of 63 beams distributed evenly in geographic space were chosen for this analysis. The ε and S indicators were estimated over subwindows of approximately 12 minutes, or equivalently approx. 500 independent STA samples. Different types of noise conditions were analyzed; quiet, normal and noisy (Table 1). Artificial coloring of the noise was obtained by using different types of bandpass filters. Although the calculation performed is simple, it is very time-consuming as we had to utilize a modified, off-line version of the on-line signal detector. For example, the analysis of one hour of real-time data required approx. six hours of computer time.

Table 1. Data used in the analysis

Data set	Time intervals (Year 1972)	Typical LTA within freq.band 1.2–3.2 Hz	Bandpass filtering[a]
1	276/17/15 – 276/18/05	80	A, B, C
	278/21/55 – 278/22/45	200	A, B, C
	279/16/45 – 279/17/30	140	A, B, C
2	239/23/00 – 240/01/45	77	A, B, D
	240/04/00 – 240/07/16	80–110	A, B, D
3	271/09/00 – 271/12/50	230	A, B, D

[a] Bandpass filters (Hz): 1.2–3.2 (A), 1.4–3.4 (B), 1.6–3.6 (C), 2.0–4.0 (D)

In Table 2 the ε-values which were measured from the STA time traces are presented. The variation in ε is very small and discloses little or no dependence on the noise conditions, filters used and the indicator. Cartwright and Longuet-Higgins (1956) assume a Gaussian distribution function for the waveform amplitudes in their model. The importance of this assumption is not known, but it is certainly violated by the distribution function of the STA-values. A Kolmogorov-Smirnov test here gave mostly Rayleigh or lognormal distributions in different STA-trace intervals. Further evidence for the skewness in the STA-distribution is the fact that the threshold value TH is far out on the tail of the STA distribution function, as indicated earlier.

Table 2. Cartwright and Longuet-Higgins (1956) ε-parameter observations for different noise situations and different bandpass filters

Time interval (1972) (day/hour/min)	Bandpass filter (Hz)					
	1.2–3.2		1.6–3.6		2.0–4.0	
	min	max	min	max	min	max
239/23/00 – 240/01/45	0.812	0.826	0.822	0.830	0.711	0.767
240/04/00 – 240/07/16	0.812	0.836	0.806	0.830	0.687	0.716
271/09/00 – 271/12/50	0.822	0.840	0.835	0.871	0.788	0.832

The results of the stability measurements for the data analyzed for different noise conditions are shown in Fig. 5. The effect of bandpass filtering on the noise stability is striking, but not unexpected from physical considerations. The point is that the probability of constructive interference between randomly phased and amplitude-modulated waves is smaller for high frequency than for low frequency wave trains. Fig. 6 shows the false alarm rate as function of the stability parameter for four different detection threshold values. The false alarm rate is defined as the sum of all detections reported to have an STA/LTA ratio larger than 8.5, 9.0, 9.5 and 10.0 dB respectively. To safeguard against weak signals in the noise samples, values of STA/LTA larger than 10.5 dB were assumed to be 'true' signal detections and henceforth removed from the sample population. It is noteworthy that the noise stability-false alarm relationship is apparently independent of whether the noise field varies artificially, using bandpass filters, or naturally.

The results of Fig. 6 may be used to find a mathematical relation between detection threshold (TH), false alarm rate (FA) and noise stability (S). A reasonable approach would be to apply a two-dimensional linear regression analysis, considering TH as a linear function of log FA and S. The reason for choosing FA and S as independent variables is that in practical application, the question of interest is what value of TH would correspond to a predetermined false alarm rate for a certain value of S. The least square fit gave:

$$\mathrm{TH(dB)} = 12.08 - (0.89 \pm 0.01) \cdot \log \mathrm{FA} - (0.18 \pm 0.02) \cdot \mathrm{S} \qquad (7)$$

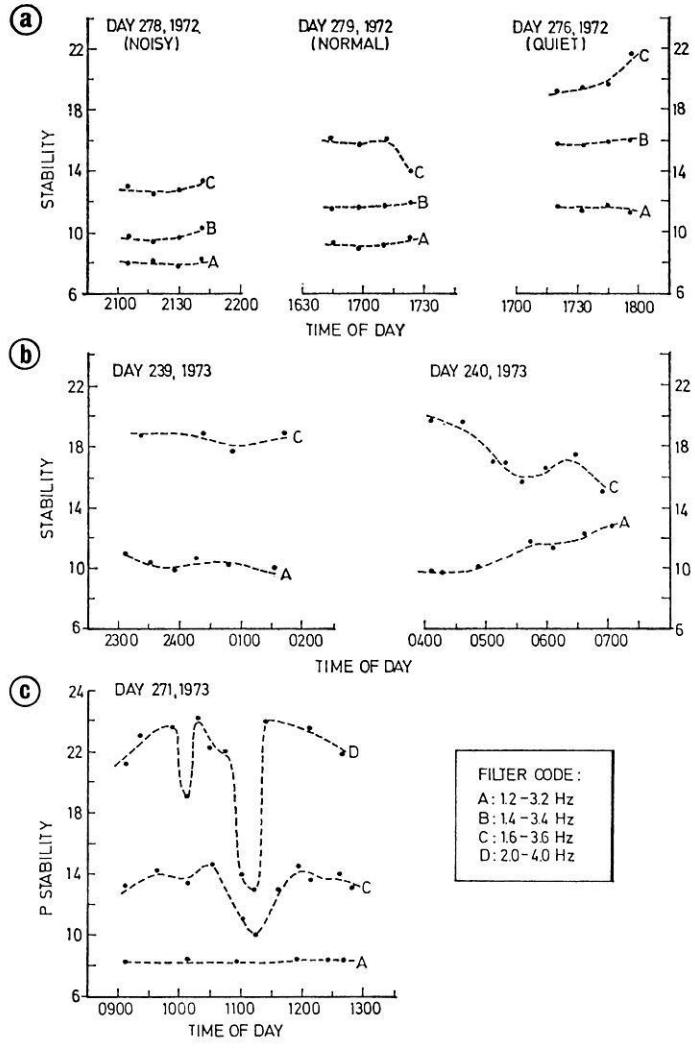

Fig. 5. Variation of stability with local time of day for different noise situations and different bandpass filters

This relation makes it possible to fix the false alarm rate and let the threshold vary as a function of noise stability. In the Appendix it is shown that the expected signal detectability R of a floating threshold procedure, relative to one with a fixed threshold, is given by

$$R = \frac{\sum_{i=1}^{M} (N_{si} \cdot N_{ni}^{-k}) \left(\sum_{i=1}^{M} N_{ni} \right)^k}{M^k \cdot \sum_{i=1}^{M} N_{si}} \tag{8}$$

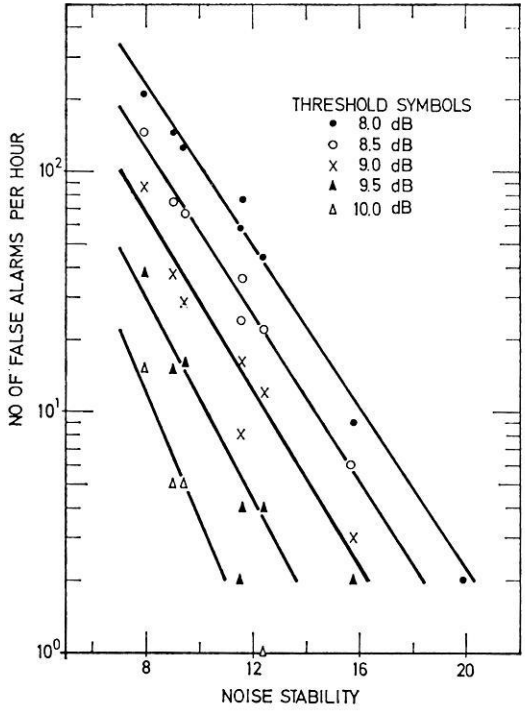

Fig. 6. False alarm rate as a function of noise stability for different values of detection threshold

where N_{si} and N_{ni} are samples of the signal and noise detection frequencies in a time interval with M samples, and k is the ratio of the slopes of the lines describing the signal and noise detection frequencies.

In order to estimate the coefficient R, we need models giving typical variations of N_s and N_n with time. Roughly, the noise variation may be divided into two parts, namely, the seasonal variation due to microseismic storm activity and the short-term variation due to diurnal fluctuations of the cultural noise. These two phenomena will have totally different effects on the noise stability. In the first case the energy increases in the low frequency range (decreasing stability) and in the second one energy increases in the high frequency range (increasing stability). In the latter case, the diurnal components of the signal and noise detection rates (N_s and N_n) will be approximately in phase (see Fig. 4), while the seasonal variations involving significant fluctuations in the LTA-level imply a phase difference of 180 degrees (Bungum and Ringdal, 1974). We use the following simple models for the variations of N_s and N_n for the i-th sample:

$$\begin{aligned} N_{si} &= A_s + B_s \cos\left(2\pi \frac{i}{M} + \phi_s\right) \\ N_{ni} &= A_n + B_n \cos\left(2\pi \frac{i}{M} + \phi_n\right) \end{aligned} \tag{9}$$

For simplicity the diurnal and seasonal noise effects on R are estimated separately. In the first case the two cosine functions are in phase (see Eq. (9)) and thus $\phi_s = \phi_n = 0$. In the second case we have $\phi_s = 0$, $\phi_n = \pi$. To estimate the coefficients A_s, B_s, A_n and B_n we need to know the relative fluctuations of signal and noise detection rates. This information may be deduced directly from Fig. 4. As to the seasonal variations, similar results are available from rough studies of signal and noise detection rates during noisy and quiet time intervals. The relative fluctuations of N_s and N_n together with the corresponding coefficients A_s, B_s, A_n and B_n are given in Table 3. From Eq. (9), N_{st} and N_{nt} were calculated and substituted into Eq. (8) to get final estimates of R for different values of k-parameter. The results obtained (see Table 4) indicate a small but significant improvement in the average signal detectability when using a floating threshold as compared to a fixed threshold detector of the type considered here. This is especially true when considering the seasonal variations in noise level, as in this case the threshold value is set too high in order to avoid system saturation during extreme noise conditions. In practice, this means that the false alarm rate is approximately zero during day time over an extended period of time. A value of k of the order 0.1 is reasonable (Bungum and Ringdal, 1974) and gives an R factor equal to about 1.04. As expected the floating threshold is especially favorable in the seasonal case, sinde these variations cause high stability (and thereby allow for low thresholds) when the LTA-level is low, whereas the opposite is true for the diurnal variations.

Table 3. Table showing typical relative variations in signal and noise detection rates, together with coefficients A_s, B_s, A_n and B_n of Eq. (9). For simplicity, A_s and A_n are set equal to 1

Quantity	Diurnal variation	Seasonal variation
$N_{s,\max}/N_{s,\min}$	1.3	3.0
$N_{n,\max}/N_{n,\min}$	1.9	6.0
A_s, B_s	1.0, 0.13	1.0, 0.5
A_n, B_n	1.0, 0.33	1.0, 0.7

Table 4. Table showing the relative gain factor R for different values of the ratio k. Values are obtained separately for a typical diurnal and a typical long term variation

k	Diurnal variation	Seasonal variation
1.0	1.04	1.7
0.5	1.01	1.2
0.1	1.001	1.04
0.05	1.0004	1.02
0.01	1.00006	1.004

Discussion

The physical operations involved in the NORSAR event detection processing are bandpass filtering for removal of low-frequency noise, then rectification which is roughly equivalent to a doubling of the signal frequency, and finally, the STA-estimation which removes most of the highfrequency signal components (see Fig. 2). The STA operation is not a perfect lowpass filter, so the high-frequency componente would be folded into the STA-spectrum (aliasing effects) as the STA sampling rate is 2 Hz. Moreover, the bandpass filter will allow low-frequency energy to leak into the filter passband. The latter effect is most pronounced during microseismic storms but in general seems to be less important than the cultural noise generated during the daily working hours. In short, variations in the ambient noise field would change the STA-spectra and henceforth its variance, as quantitatively demonstrated in Fig. 5. The removal of low-frequency noise gives better stability values, i.e., a smaller false alarm rate. However, for the extremely high-frequency filters, the stability parameter becomes less stable again, probably due to short time fluctuations in the cultural noise and the narrowness of the corresponding noise spectra.

A large data base covering time periods where the change in cultural background noise has been observed to be largest, i.e., early morning and evening during work days, would have been advantageous, but only one such period is presented. For Day 240, Fig. 5 shows that the noise stability increases with time for the 1.2—3.2 Hz filter. This filter is currently used in the NORSAR detection processor, and the time of day analyzed is that for which Fig. 4 shows the most rapid decrease in the false alarm rate.

From the above discussion we conclude that the stability parameter represents a useful false alarm rate indicator. On the other hand, the ε-parameter seems to be for all practical purposes independent of changes in the noise field and/or the bandpass filter in use, and in consequence is not useful as a false alarm rate indicator.

It is appropriate to comment on the potential gain when the false alarm rate of the detector is kept approximately constant by using a floating threshold value. The false alarm indicator and the associated threshold value estimator defined in Eqs. (6) and (7) have not yet been implemented in the NORSAR on-line detector. However, as a first approximation to control the false alarm rate on a diurnal basis we have implemented a predefined, sinusoidal TH-parameter variation as a function of local time of day. The amplitude of this function, determined on the basis of the noise character of the five work days of the week, is 0.075 units, corresponding to a maximum value of TH at night time of around 3.70 and a minimum value of TH at day time of around 3.55. Preliminary analysis of the false alarm rate after implementation of the above TH-function shows that it has been successful in removing a large part of the diurnal effect.

We remark that the floating threshold procedure has advantages besides that of controlling the false alarm rate and the expected increase in signal detectability. For example, Bungum and Ringdal (1974) pointed out that the considerable diurnal variation in signal detection rate (see Fig. 4) could not be fully explained by the modest fluctuation in noise level (see also Shimshoni, 1972). They proposed that a possible explanation might be a tendency to accept more noise detections as signals when the false alarm rate is high and vice versa, accounting for the good correlation between

the two curves of Fig. 4. Obviously, using a floating threshold would tend to eliminate such an unwanted effect, as the false alarm rate would not be subject to diurnal fluctuations. The underlying assumption is, of course, that earthquake occurrence is independent of local time of day (e.g., see Davis, 1972; Flinn *et al.*, 1972; and Knopoff and Gardner, 1972).

Finally, it is not clear whether the result presented above is valid for signal detections based on visual inspections of ordinary seismograms. However, noise spectra variations would, if not accounted for, significantly affect the global network detectability of small earthquakes because large seismic arrays NORSAR and LASA contribute significantly to the seismicity of the earth as reported by NOAA and similar agencies.

Conclusions

In this paper it is demonstrated that noise variance fluctuations besides those of noise level fluctuations also affect our capability to detect small earthquakes when an automatic seismic signal detector is utilized. The importance of maximizing this detectability in surveillance and other seismological studies needs no further emphasis here. The advantages of a floating threshold detector as compared to a fixed threshold detector are an increase in the average signal detectability, an approximately constant number of false alarms per unit time in the detector system, and avoidance of system saturation during extremely noisy periods which otherwise could only be obtained by using an overly conservative threshold level.

Acknowledgement. This research was supported by the Advanced Research Projects Agency of the U. S. Department of Defense and was monitored by AFTAC/VSC, Patrick AFB FL 32925, under Contract No. F 0860674C0049.

Appendix

Evaluation of Signal Detectability Using Fixed and Floating Detection Thresholds

The earthquake frequency-magnitude distribution of NORSAR may be described by a straight line as shown in Fig. 7 (Bungum and Husebye, 1974). Thus, the signal detection rate of NORSAR, N_s, may be tied directly to this functional relationship, namely,

$$\log N_s = b_s \cdot \mathrm{TH} + a_s \tag{A1}$$

where the slope b_s is approximately —1.

The relationship between the noise detection frequency, N_n, and the detection threshold is given by Eq. (7):

$$\log N_n = b_n \cdot \mathrm{TH} + a_n \text{ where } a_n = c_n \cdot \mathrm{S} + d_n \tag{A2}$$

The above signal-noise detection model is demonstrated in Fig. 7, and will be used for a functional comparison of the signal detection performance of the STA/LTA-detector using fixed and floating threshold values. It is required that N_{tot},

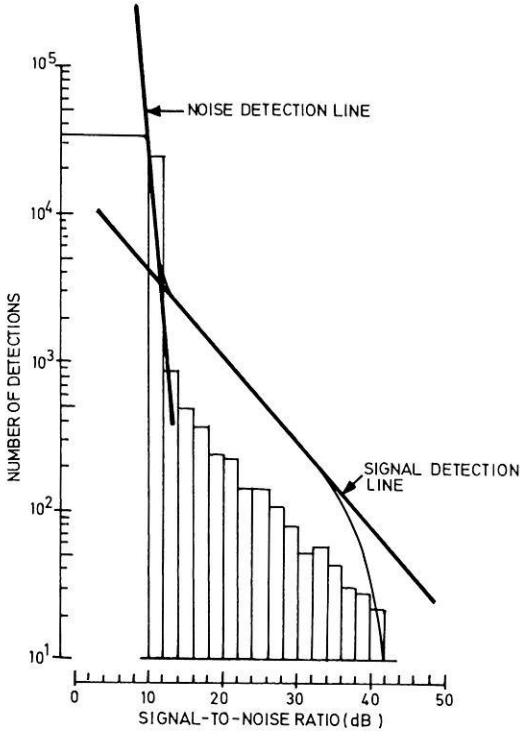

Fig. 7. Incremental and cumulative distribution of number of detections as a function of SNR. The data is from the time period July-December 1972. (After Bungum and Ringdal 1974)

i.e., the total number of acceptable false alarms within an interval T, is the same for the two threshold settings considered.

The number of signal detections N_{fix} and N_{fl} for fixed and floating threshold values in the interval T can be estimated from Eqs. (A1) and (A2). For fixed threshold values we have:

$$N_{\text{fix}} = N_{\text{tot}}^k \left(\int_0^T 10^{a_s(t)}\, dt \right) \left(\int_0^T 10^{a_n(t)}\, dt \right)^{-k} \quad k = b_s/b_n \tag{A3}$$

and for floating threshold values:

$$N_{\text{fl}} = \left(\frac{N_{\text{tot}}}{T} \right)^k \cdot \int_0^T 10^{a_s(t) - k \cdot a_n(t)} dt \tag{A4}$$

If N_s and N_n were known for a certain fixed threshold, the functions a_s and a_n can be estimated from (A1) and (A3). From (A3) and (A4), we get

$$N_{\text{fix}} = N_{\text{tot}}^k \left(\int_0^T N_s(t)\, dt \right) \cdot \left(\int_0^T N_n(t)\, dt \right)^{-k} \tag{A5}$$

$$N_{\mathrm{fl}} = \left(\frac{N_{\mathrm{tot}}}{T}\right)^{k} \cdot \int_{0}^{T} N_s(t)\, N_n(t)^{-k}\, dt \tag{A6}$$

Considering N_s and N_n as discrete functions of time, and choosing the number of false alarm rate samples in the time interval T equal to M we may write:

$$R = \frac{N_{\mathrm{fl}}}{N_{\mathrm{fix}}} = \frac{\sum_{i=1}^{M} (N_{si} N_{ni}{}^{-k}) \left(\sum_{i=1}^{M} N_{ni}\right)^{k}}{M^{k} \sum_{i=1}^{M} N_{si}} \tag{A7}$$

Note that only the relative variation of N_s and N_n with time must be known, as any constant multiplication factor from Eqs. (A5) and (A6) will vanish in Eq. (A7). For this reason, when estimating the N_s and N_n functions, it is not necessary to refer to the same threshold.

References

Bungum, H., Husebye, E. S., Ringdal, F.: The NORSAR array and preliminary results of data analysis. Geophys. J. *25*, 115–126, 1971

Bungum, H., Husebye, E. S.: Analysis of the operational capabilities for detection and location of seismic events at NORSAR. Bull. Seism. Soc. Am. *64*, 637–656, 1974

Bungum, H., Ringdal, F.: Diurnal variation of seismic noise and its effect on detectability. NORSAR Scientific Report No. 5–73/74, NTNF/NORSAR, Kjeller, Norway, 1974

Cartwright, D. E., Longuet-Higgins, M. S.: The statistical distribution of the maxima of a random function. Proc. Roy. Soc. (London) Ser. A. *237*, 212–232, 1956

Davies, D.: Nocturnal earthquakes. Geophys. J. *28*, 305, 1972

Flinn, E. A., Blandford, R. R., Mack, H.: Comments on 'Evidence for higher seismic activity during the night', by Michael Shimshoni. Geophys. J. *28*, 307–309, 1972

Helstrom, C. W.: Statistical theory of signal detection. Oxford: Pergamon Press 1968

Knopoff, L., Gardner, J. K.: Higher seismic activity during local night on the raw worldwide earthquake catalogue. Geophys. J. *28*, 311–313, 1972

Lacoss, R. T.: Variation of false alarm rates at NORSAR. Semiannual Technical Summary. Seismic Discrimination, M.I.T. Lincoln Lab, Mass. Inst. of Tech., Cambridge, Mass., June 1972, 53–57, 1972

Rice, S. O.: Mathematical analysis of random noise. Bell System Tech. J., *23*, 282–332, 1944

Shimshoni, M.: Evidence for higher seismic activity during the night. Geophys. J. *24*, 97–99, 1971

Shimshoni, M.: Response to comments by Davies, by Flinn *et al.* and by Knopoff *et al.* on the 'Evidence for higher seismic activity during the night'. Geophys. J. *28*, 315, 1972

Ole Steinert
Eystein S. Husebye
Håvar Gjøystdal
NTNF/NORSAR
Post Box 51
N-2007 Kjeller, Norway